Tensile Behavior of Functionally Graded Steels Produced by Electroslag Remelting

J. AGHAZADEH MOHANDESI, M.H. SHAHOSSEINIE, and R. PARASTAR NAMIN

Tensile behavior of functionally graded steels produced by electroslag refining has been studied. Functionally graded steels containing layers of ferrite, austenite, bainite, and martensite may be fabricated *via* diffusion of alloying elements during electroslag remelting. Tensile strength of the composites depends on the composition and number of layers and those have been modeled based on the tensile behavior of individual phases. The yield stress of each element in the composites is related to the microhardness value of that element. Considering the Holloman relation for the true stress-strain behavior of each element, the tensile strength of an individual element is also related to the microhardness value of that element. By applying the rule of mixtures, the tensile strengths of the composites were determined *via* the numerical method. The obtained results are in good agreement with the experimental results.

I. INTRODUCTION

ALTHOUGH considerable attention has been drawn to produce functionally graded materials (FGMs),[1,2] it seems that the utility of FGMs with metallic base is yet to be investigated. Functionally graded steels (FGSs) were originally produced from austenitic stainless steel and carbon steel base materials using electroslag remelting.[3] Microstructural studies of the FGSs have shown that it is possible to obtain multilayered composites consisting of ferrite, austenite, bainite, and martensite. By selecting the appropriate arrangement and thickness of the initial ferritic and austenitic steels used to set up the electrodes, it is possible to control the variety and thickness of the merging phases after remelting. When the primary electrode contains two slices of ferritic and austenitic layers as $(\alpha_0\gamma_0)$, the morphology of the resultant composite is $(\alpha\beta\gamma)$; hence,

$$(\alpha_0\gamma_0)_{el} \xrightarrow{R} (\alpha\beta\gamma)_{\text{com}}$$

where

α = ferretic layer,
γ = austenitic layer,
β = bainitic layer,
el = electrode,
com = composite, and
R = remelting.

Similarly, when the primary electrodes contain three slices of ferretic and austenitic steels, the following phases appear in the final composite after remelting:

$$(\alpha_0\gamma_0\alpha_0)_{el} \xrightarrow{R} (\alpha\beta\gamma\beta\alpha)_{\text{com}}$$

$$(\gamma_0\alpha_0\gamma_0)_{el} \xrightarrow{R} (\gamma M\gamma)_{\text{com}}$$

where M = martensitic layer.

Finally, by using four slices of austenitic and ferretic steels, it follows that

$$(\alpha_0\gamma_0\alpha_0\gamma_0)_{el} \xrightarrow{R} (\alpha\beta\gamma M\gamma)_{\text{com}}$$

$$(\gamma_0\alpha_0\alpha_0\gamma_0)_{el} \xrightarrow{R} (\gamma\beta\alpha\beta\gamma)_{\text{com}}$$

Diffusion of chromium, nickel, and carbon atoms taking place at the remelting stage in the liquid phase controls the chromium, nickel, and carbon atom distribution pattern in the produced composites. As alloying elements diffuse, alternating regions with different transformation characteristics are created. The diffusing atoms individually or together stabilize different phases such as bainite or martensite. The transformation characteristics of FGSs have already been presented.[3] In this work, the tensile behavior of these composites is studied.

II. EXPERIMENTAL METHOD

An experimental electroslag remelting apparatus was set up to produce FGSs. A mixture of 20 pct CaO, 20 pct Al_2O_3, and 60 pct CaF_2 was used as the slag. Consumable electrodes consist of slices of AISI 1020 and AISI 316 steels (called alfa, α_0 and gamma, γ_0 steel in this work, respectively) with chemical compositions as given in Table I. The height of slices was 25 mm in four-piece, 50 mm in two-piece, and 25 mm and (37.5 × 2) mm in three-piece electrodes.

The remelting procedure was carried out under a constant power supply of 16 kVA. Cylindrical specimens with up to four layers of alfa and gamma steels were fabricated, upset, and finally hot rolled into plates of multilayered composites. Rolling and forging operations were carried out at 980 °C, and then the plates were air cooled. Vickers microhardness tests were conducted using one kgf weight.

Tensile tests were carried out under an extension rate of 0.1 m/s. Specimen dimensions are in accordance with the ASTM E8 standard, as shown in Figure 1. The longitudinal direction of the tensile specimens was parallel to the rolling

J. AGHAZADEH MOHANDESI, Associate Professor, and R. PARASTAR NAMIN, Postgraduate Research Student, are with the Department of Mining and Metallurgical Engineering, Amir Kabir University of Technology, Tehran, Iran. Contact e-mail: agazad@yahoo.com or agazad@aut.ac.ir M.H. SHAHOSSEINIE, Assistant Professor, is with the Faculty of Engineering, Department of Metallurgy, University of Tehran, Tehran, Iran.

Manuscript submitted August 29, 2005.

Table I. Chemical Composition of Gamma and Alfa steels

Steel	Pct C	Pct Si	Pct Mn	Pct P	Pct S	Pct Cr	Pct Ni
Gamma (γ_0)	0.07	1	2	0.045	0.03	18.15	9.11
Alfa (α_0)	0.2	0.3	0.2	0.05	0.05	—	—

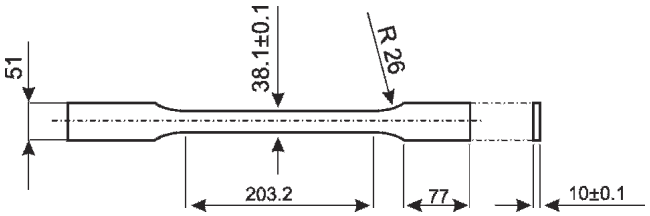

Fig. 1—Dimension of tensile composite specimen (mm).

direction, and the specimen's wider surface was parallel to the layer's interface. Also, the longitudinal direction of the tensile specimens taken from the as-received alfa and gamma steels was parallel to the rod axis. The as-received rods were annealed at 980 °C and then air-cooled.

III. RESULTS AND DISCUSSION

Microhardness profiles of the $\alpha\beta\gamma$, $\gamma M\gamma$, $\gamma\beta\alpha\beta\gamma$, $\alpha\beta\gamma M\gamma$, and $\alpha\beta\gamma\beta\alpha$ composites are shown in Figures 2 through 6, respectively; phase distribution and position of merging bainite and martensite phases are also indicated. For the purpose of modeling, the inner austenite layer in the $\alpha\beta\gamma M\gamma$ composite has been divided into three regions: γ_I, γ_{II}, and γ_{III}. In Figure 7, the microstructure of the martensitic phase surrounded by austenitic layers in the $\alpha\beta\gamma M\gamma$ composite is shown. The microstructure of the bainitic phase formed between ferretic and austenitic layers is shown in Figure 8. The thickness and microhardness of bainite and martensite layers in all studied composites were similar, since the process variables and initial base materials remained unchanged. This is in accordance with the previous work that the concentration of alloying elements of bainite and martensite phases in each of the studied composites are similar.[3] The microhardness values of each element in these functionally graded steels depend on the transformation characteristic of that element. Due to the diffusion of chromium and nickel atoms from gamma to alfa steel, and inversely carbon atoms from alfa to gamma steel, the concentration of these alloying elements in the produced composite are graded as are the microhardness profiles.[3]

A. *Modeling the Tensile Strength of Three Layered Composites*

Several aspects of FGMs have been modeled, *e.g.,* thermo-elastic-plastic behavior,[4] propagation of stress waves,[5] and residual stress.[6] Although some limited work on elastic and plastic analyses of FGMs has been conducted,[7] it seems that more studies are required to establish a correlation between the microstructure and mechanical properties of FGMs in order to obtain more realistic models.

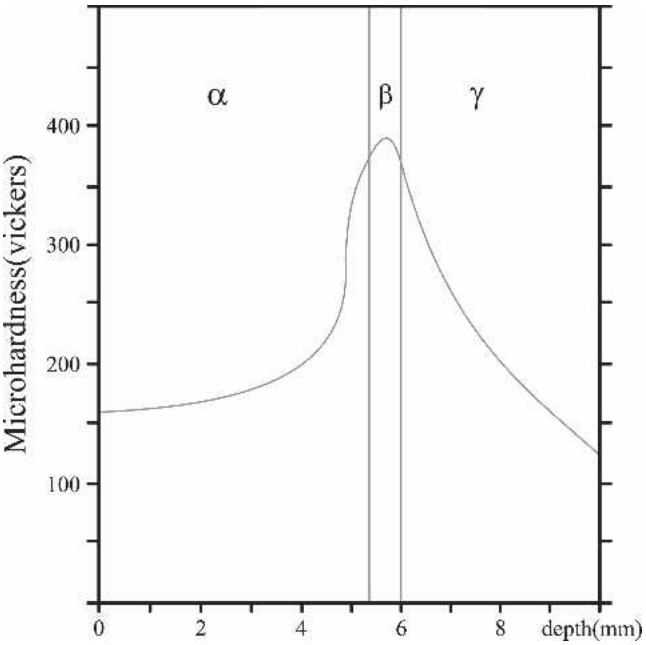

Fig. 2—Microhardness profile of $\alpha\beta\gamma$ composite plate.

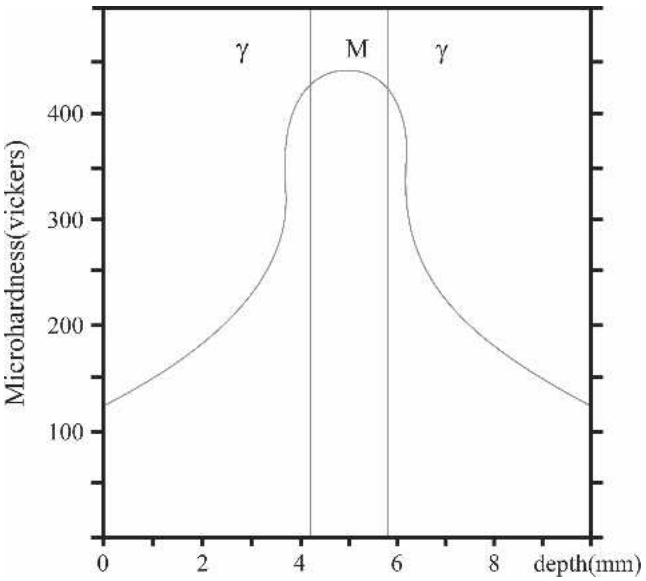

Fig. 3—Microhardness profile of $\gamma M\gamma$ composite plate.

In this work, the tensile strength of FGSs is modeled. To simulate the tensile strength of the three layered composites, tensile test specimens from a single-phase layer as thin films were delicately made out of each composite by electrodischarge machining (EDM). The positions of the specimens are selected such that each contains single-phase bainite in the $\gamma\beta\gamma$ composite and single-phase martensite in the $\gamma M\gamma$ composite (Figures 2 and 3).

Thickness of the tensile test specimens made from single phase bainite (β) and martensite (M) layers are 0.6 mm and 1.5 mm respectively. Dimensions of the tensile test specimens are shown in Figure 9. Dimensional tolerance for the obtained specimens is less than 0.033 mm.

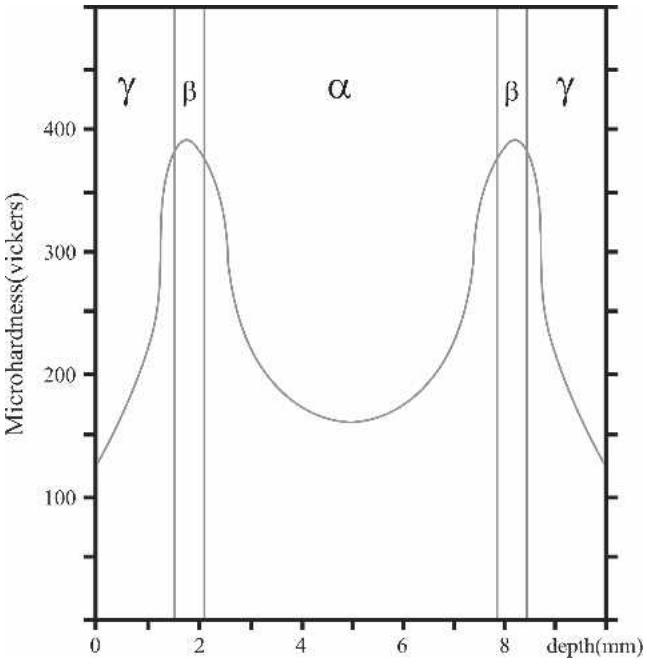

Fig. 4—Microhardness profile of $\gamma\beta\alpha\beta\gamma$ composite plate.

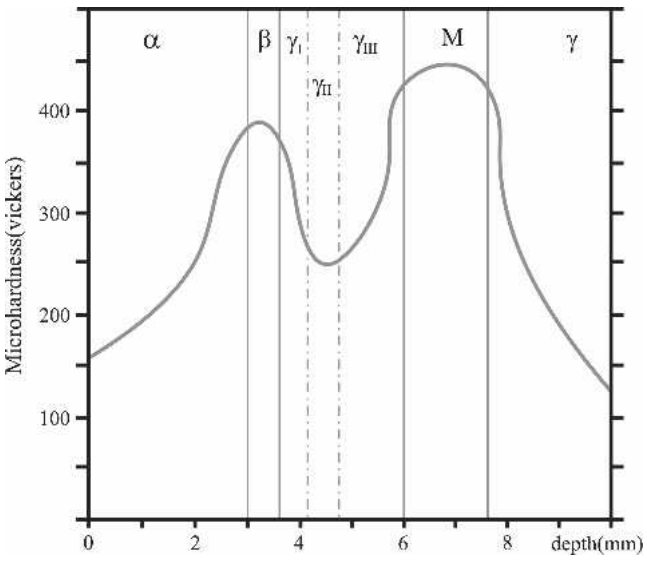

Fig. 5—Microhardness profile of $\alpha\beta\gamma M\gamma$ composite plate.

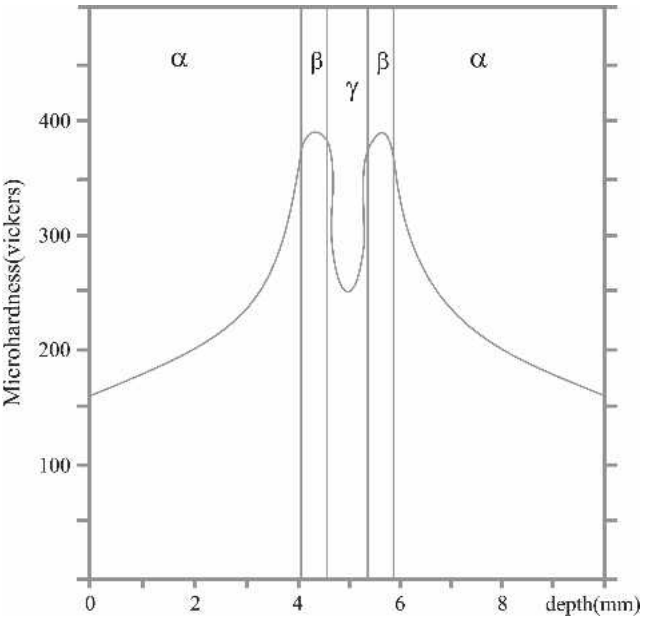

Fig. 6—Microhardness of $\alpha\beta\gamma\beta\alpha$ composite plate.

Fig. 7—Martensitic layer surrounded by austenite phase.

The thickness of the tensile composite sample is not the same as that of the individual constituent phases; therefore, the stress state within the thinner sample may be different than in the thicker samples. For the purpose of modeling the tensile strength of the composites, the stress-strain curves of the thinner constituent phases are corrected to obtain the modified stress-strain curves of the single-phase bainitic and martensitic layers; initially, the average chemical composition of the layers was obtained (Table II). Afterward, bainitic and martensitic staples with composition in accordance with the average composition of the single-phase bainitic and martensitic specimens were produced by means of a vacuum induction furnace. Similar to the primary composites, the hot rolling process was carried out at 980 °C, followed by air cooling. Through trial and error (*i.e.,* conforming the chemical composition and changing the cooling rate), the staples with the nearest hardness to the single-phase bainitic and martensitic specimens were chosen and tensile test specimens with 0.6- and 10-mm thickness and 1.5- and 10-mm thickness were made from the bainitic and martensitic staples, respectively.

Dimensions of the 0.6-mm and 1.5-mm-thick specimens are shown in Figure 9 and that of the 10-mm-thick specimen is shown in Figure 1. Tensile test results of the single-phase bainitic and martensitic layers together with those produced from the staples are shown in Table III. As seen, there is excellent agreement between the yield and tensile stresses of 0.6- and 1.5-mm single-phase specimens with those produced from the staples. Therefore, the stress-strain curves of the 10-mm bainitic and martensitic specimens may be considered as corrected stress-strain curves of single-phase bainitic and martensitic specimens, respectively. Figures 10 and 11 illustrate true stress-strain curves of the $\alpha\beta\gamma$ and $\gamma M\gamma$ composites, the corrected single-phase

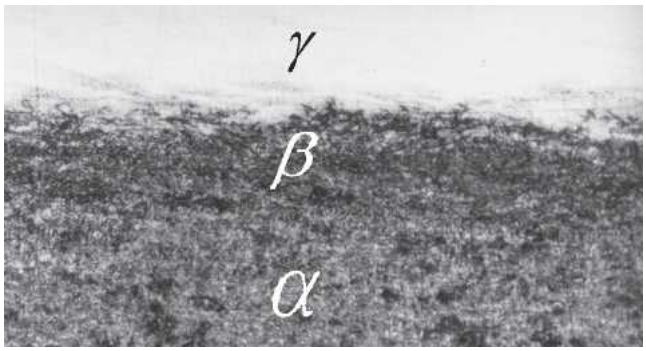

Fig. 8—Bainitic layer formed between austenite and ferrite phases.

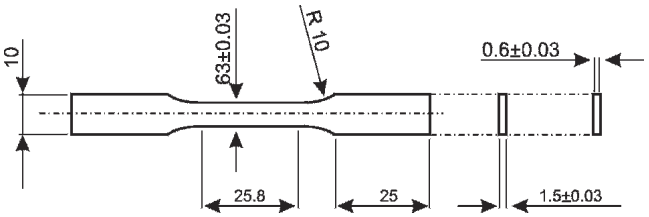

Fig. 9—Dimensions of single-phase martensite and bainite tensile specimens (mm).

specimens of bainite and martensite, together with the original alfa and gamma steels. The tensile test result of the alfa and gamma steels represents the boundary condition to the studied composites (*i.e.,* tensile behavior of the composite edge layers). Electron-probe microanalysis studies illustrate that the chemical composition of the α edge layer is pct C = 0.2, pct Cr = trace, and pct Ni = trace, and that for the γ edge layer is pct C = 0.07, pct Cr = 18.1, and pct Ni = 9.1, which is similar to that of original alfa and gamma steels; this is in accordance with the previous results.[3]

In order to model the tensile strength of $\alpha\beta\gamma$ composite, the cross section of the specimen is divided into regions of α, γ, and β (Figure 2). It is assumed that region α consists of m_α elements. The tensile strength of the constituent elements in this region changes from the original alfa steel from one side to the bainite layer at the other side. Similarly, it may be assumed that region γ consists of m_γ elements, and in this region, the tensile strength of constituent elements changes from the tensile strength of the bainite layer from one side to that of the original gamma steel at the other side. Further, it is assumed that the yield stress of each element is proportional to the Vickers microhardness of that element. Therefore, the yield stress of each element in regions α and γ should also obey the hardness pattern. Therefore, the yield stress of each element may be related to the Vickers microhardness of that element as

$$\sigma_y(\alpha_i)=VH(\alpha_i)\left[\frac{\sigma_y(\alpha_0)}{VH(\alpha_0)}+\frac{\frac{\sigma_y(\beta)}{VH(\beta)}-\frac{\sigma_y(\alpha_0)}{VH(\alpha_0)}}{m_\alpha-1}(i-1)\right]$$

$$i=1\ldots m_\alpha$$

Table II. Chemical Composition of the Bainitic and Martensitic Single Layers Together with Those of Produced Staples

Specimen Studied	Pct Cr	Pct Ni	Pct C	Pct Si	Pct Mn	Pct S	Pct P
Single-phase bainite	14.5	7.2	0.12	0.8	1.8	0.03	0.04
Single-phase martensite	7.3	3.2	0.19	0.39	0.3	0.04	0.05
Bainite specimen produced from the staple	14.7	7.15	0.13	0.85	1.9	0.032	0.045
Martensite specimen produced from the staple	7.38	3.14	0.21	0.28	0.28	0.033	0.055

Table III. Tensile Test Results of the Single-Phase Bainitic and Martensitic Layers Together with Those Produced from the Staples

Specimen Studied	Thickness (mm)	Yield Stress (MPa)	Tensile Stress (MPa)
Single-phase bainite	0.6	1451	1520
Single-phase martensite	1.5	1654	1653
Bainite specimen produced from the staple	0.6	1460	1531
	10	1025	1125
Martensite specimen produced from the staple	1.5	1662	1662
	10	1440	1482

$$\sigma_y(\gamma_i)=VH(\gamma_i)\left[\frac{\sigma_y(\gamma_0)}{VH(\gamma_0)}+\frac{\frac{\sigma_y(\beta)}{VH(\beta)}-\frac{\sigma_y(\gamma_0)}{VH(\gamma_0)}}{m_\gamma-1}(i-1)\right]$$

$$i=1\ldots m_\gamma$$

where $\sigma_y(\beta)$, $\sigma_y(\alpha_0)$, and σ_y (γ_0) = yield stresses of the bainite layer, alfa steel, and gamma steel, respectively; $VH(\alpha_i)$ = Vickers microhardness of each element; $VH(\alpha_0)$, $VH(\gamma_0)$ = Vickers microhardness of alfa and gamma steels, respectively; and m_α, m_γ = number of elements in regions α and γ, respectively.

If it is assumed that the stress-strain curve of each element obeys the Holloman relation, the imposed stress to each element at fracture strain of the composite may be given as

$$\sigma'_i=\sigma_y(\alpha_i)\left[\frac{\varepsilon'}{\varepsilon(\alpha_i)}\right]^{n(\alpha_i)}$$

$$\sigma''_i=\sigma_y(\gamma_i)\left[\frac{\varepsilon'}{\varepsilon(\gamma_i)}\right]^{n(\gamma_i)}$$

where σ'_i, σ''_i,= imposed stress to each element in the α and γ regions at the fracture strain of the composite; ε' = fracture strain of the composite; and $n(\alpha_i)$ and $n(\gamma_i)$ = strain-hardening coefficient of each element in regions α and γ, respectively. It is assumed that the stain hardening coefficient of each element within the studied region of the composite obeys exponential functions; therefore,

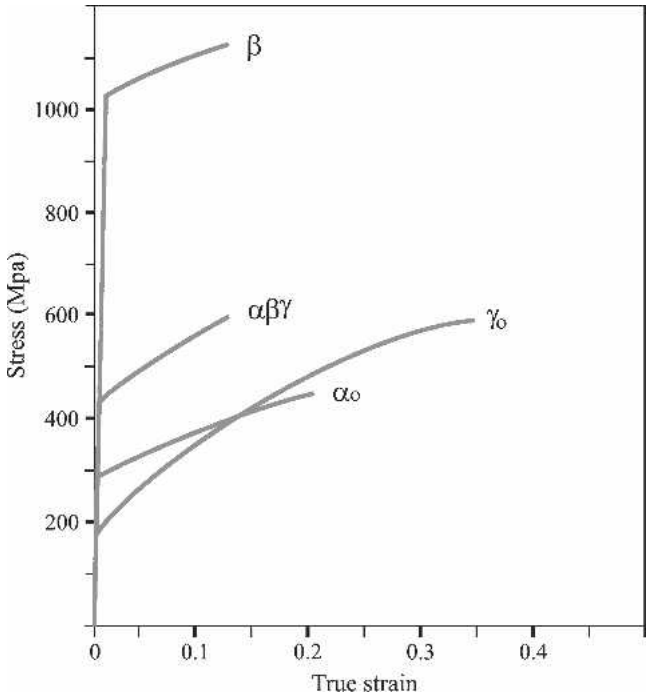

Fig. 10—True stress-strain curves of $\alpha\beta\gamma$ composite, single phase of bainite, alfa, and gamma steels.

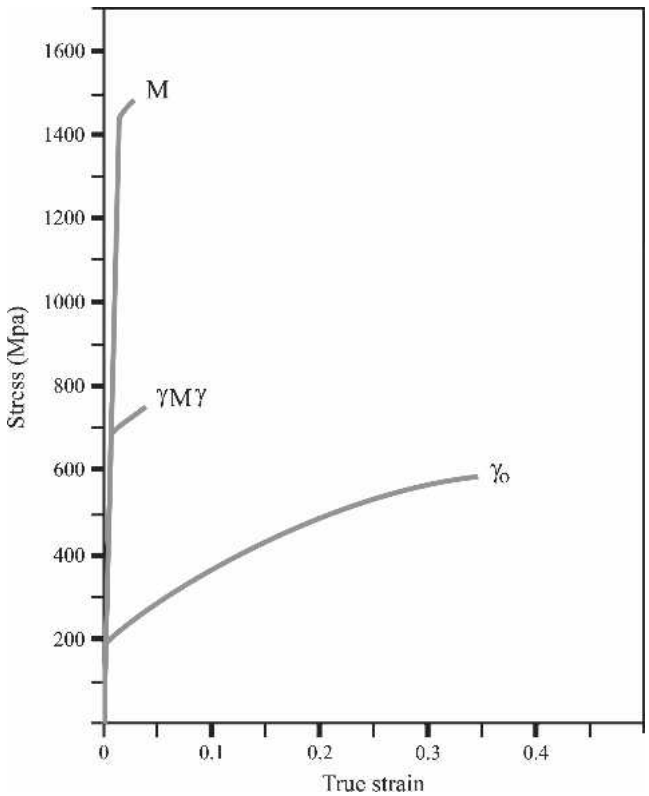

Fig. 11—True stress-strain curves of $\gamma M\gamma$ composite, single phase of martensite and gamma steel.

$$n(\alpha_i)=n(\alpha_0)\ \exp\left[\frac{\ln\dfrac{n(\beta)}{n(\alpha_0)}}{m_\alpha-1}(i-1)\right]$$

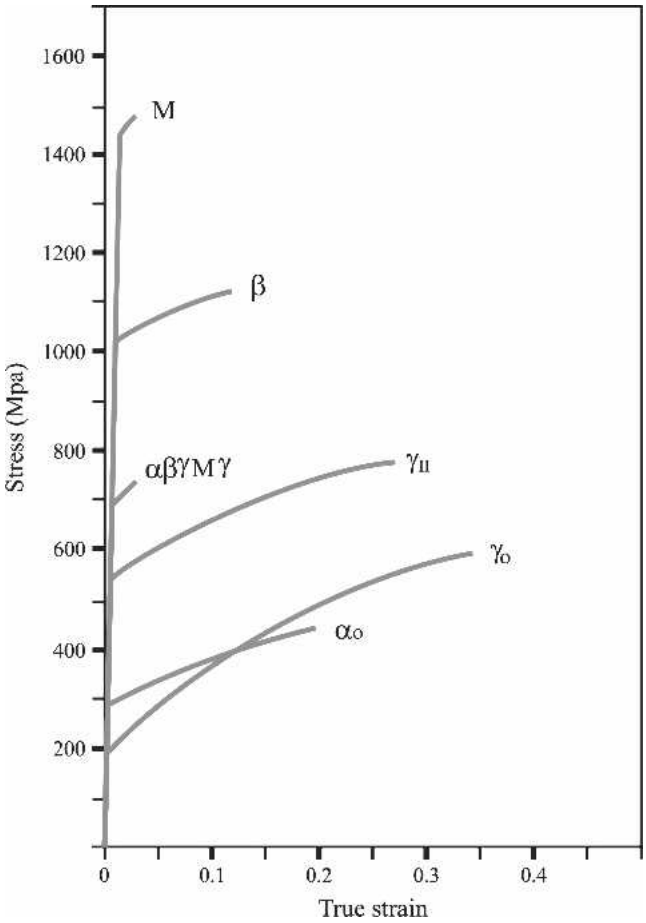

Fig. 12—True stress-strain curves of $\alpha\beta\gamma M\gamma$ composite, single phase of bainite, martensite, austenite, alfa, and gamma steels.

$$n(\gamma_i)=n(\gamma_0)\ \exp\left[\frac{\ln\dfrac{n(\beta)}{n(\gamma_0)}}{m_\gamma-1}(i-1)\right]$$

where $n(\alpha_0)$, $n(\gamma_0)$, and $n(\beta)$ = strain-hardening coefficient of the alfa steel, gamma steel, and bainite layer, respectively; and $\varepsilon(\alpha_i)$ and $\varepsilon(\gamma_i)$ in Eqs. [3] and [4] are defined as the yield strain of each element in regions α and γ, respectively.

By considering the boundary conditions,

At $i = 1$, $\varepsilon(\alpha_i) = \varepsilon(\alpha_0)$

At $i = m_\alpha$, $\varepsilon(\alpha_i) = \varepsilon(\beta)$

Similarly,

At $i = 1$, $\varepsilon(\gamma_i) = \varepsilon(\gamma_0)$

At $i = m_\gamma$, $\varepsilon(\gamma_i) = \varepsilon(\beta)$

where

$\varepsilon(\alpha_0)$, $\varepsilon(\gamma_0)$, and $\varepsilon(\beta)$ = yield strain of the alfa steel, gamma steel, and bainitic layer respectively.

The yield strain of each element in regions α and γ of the composite is as follows:

$$\varepsilon(\alpha_i)=\frac{VH(\alpha_i)}{E}\left[\frac{\sigma_y(\alpha_0)}{VH(\alpha_0)}+\frac{\dfrac{\sigma_y(\beta)}{VH(\beta)}-\dfrac{\sigma_y(\alpha_0)}{VH(\alpha_0)}}{m_\alpha-1}(i-1)\right]$$

$i=1\ldots m_\alpha$

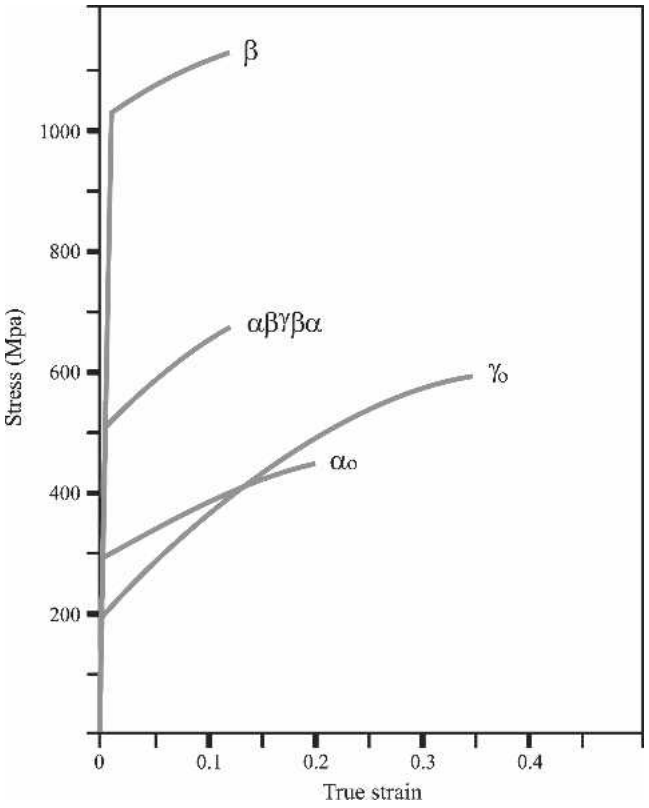

Fig. 13—True stress-strain curves of $\alpha\beta\gamma\beta\alpha$ composite, single phase of bainite, alfa, and gamma steels.

$$\varepsilon(\gamma_i)=\frac{VH(\gamma_i)}{E}\left[\frac{\sigma_y(\gamma_0)}{VH(\gamma_0)}+\frac{\frac{\sigma_y(\beta)}{VH(\beta)}-\frac{\sigma_y(\gamma_0)}{VH(\gamma_0)}}{m_\gamma-1}(i-1)\right]$$

$$i=1\ldots m_\gamma$$

where E = elastic modulus.

Now considering σ'_β as the tensile strength of the bainite layer, by combining Eqs. [1] through [6], the tensile strength of the $\alpha\beta\gamma$ composite may be determined by using the rule of mixtures as following:

$$\begin{aligned}\sigma_{ts}(\alpha\beta\gamma) = &\sum_{i=1}^{m_\alpha} VH(\alpha_i)\left[\frac{\sigma_y(\alpha_0)}{VH(\alpha_0)}+\frac{\frac{\sigma_y(\beta)}{VH(\beta)}-\frac{\sigma_y(\alpha_0)}{VH(\alpha_0)}}{m_\alpha-1}(i-1)\right]\\ &\left[\frac{\varepsilon'}{\varepsilon(\alpha_i)}\right]^{n(\alpha_i)} V_i\\ &+\sum_{i=1}^{m_\gamma} VH(\gamma_i)\left[\frac{\sigma_y(\gamma_0)}{VH(\gamma_0)}+\frac{\frac{\sigma_y(\beta)}{VH(\beta)}-\frac{\sigma_y(\gamma_0)}{VH(\gamma_0)}}{m_\gamma-1}(i-1)\right]\\ &\left[\frac{\varepsilon'}{\varepsilon(\gamma_i)}\right]^{n(\gamma_i)} V_i+\sigma'(\beta)V(\beta)\end{aligned}$$

where V_β = volume fraction of bainite phase, and V_i = volume fraction of each element in α and γ region.

Because necking was not observed in the martensite specimen and in the bainitic specimen, that was not very remarkable, to the first approximation, it is assumed that the Holloman relation is valid up to the fracture point. For the purpose of numerical determination of tensile strength of $\alpha\beta\gamma$ composites, it is assumed that the thickness of each element in regions α and γ is 10 μm (*i.e.,* in this case, the maximum difference in the strength of two adjacent elements is less than 8 MPa). By taking into account the thickness of regions α and γ, the number of elements in each region (m_α, m_γ) may be obtained. The strain-hardening coefficients of the boundary elements, $n(\alpha_0)$, $n(\gamma_0)$, and $n(\beta)$, were determined from the corresponding stress-strain curves. Since the Holloman relation is not fully satisfied (*i.e.,* the slopes of ln σ against ε are not constant), mean values for the strain-hardening coefficient were considered. This is consistent with the previous results obtained for mild steels[8] and austenitic stainless steels.[9] Finally, by using the microhardness value of each element and those of bainite, alfa, and gamma steels, the tensile strength of the $\alpha\beta\gamma$ composite is numerically determined. The result is shown in Table IV.

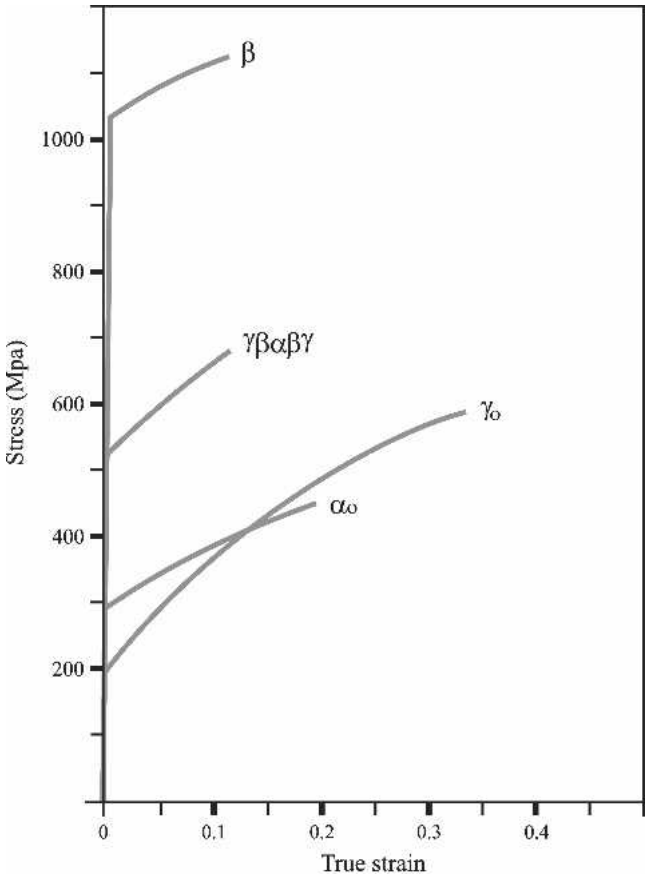

Fig. 14—True stress-strain curves of $\gamma\beta\alpha\beta\gamma$ composite, single phase of bainite, alfa, and gamma steels.

Similarly, the tensile strength of the $\gamma M\gamma$ composite may be presented as follows:

$$\begin{aligned}\sigma_{ts}(\gamma M\gamma)=2\sum_{i=1}^{m_\gamma} VH(\gamma_i)&\left[\frac{\sigma_y(\gamma_0)}{VH(\gamma_0)}+\frac{\frac{\sigma_y(M)}{VH(M)}-\frac{\sigma_y(\gamma_0)}{VH(\gamma_0)}}{m_\gamma-1}(i-1)\right]\\ &\left[\frac{\varepsilon'}{\varepsilon(\gamma_i)}\right]^{n(\gamma_i)} V_i+\sigma'(M)V(M)\end{aligned}$$

where σ'_M = tensile strength of the martensite layer, and ν_M = volume fraction of the martensite layer.

The tensile strength of the $\gamma M\gamma$ composite was numerically determined and the result is shown in Table IV. As seen, the agreement between the obtained and experimental results for three layer composites is considerable.

B. *Modeling the Tensile Strength of Five- and Six-Layered Composites*

In Figures 12 through 14, the stress-strain curves of $\alpha\beta\gamma M\gamma$, $\alpha\beta\gamma\beta\alpha$, and $\gamma\beta\alpha\beta\gamma$ composites are shown.

Since in $\alpha\beta\gamma M\gamma$ composite the microhardness profile in the austenitic region between bainite and martensite layers reaches a minimum value, to model the $\alpha\beta\gamma M\gamma$ composite, it is essential to take into account the tensile behavior of this austenitic layer (γ_{II}). Therefore, a 0.6-mm-thick tensile test specimen was delicately made by EDM from this region of the composite. Given the average concentration of the γ_{II} as pct Cr = 16.1, pct Ni = 8.06, pct C = 0.08, pct Mn = 1.9, pct p = 0.04, and pct S = 0.03, the stress-strain curve of the γ_{II} layer is also corrected and that is shown in Figure 12. The yield stresses of each element in regions α, γ_I, γ_{III}, and γ are

$$\sigma_y(\alpha_i)=VH(\alpha_i)\left[\frac{\sigma_y(\alpha_0)}{VH(\alpha_0)}+\frac{\frac{\sigma_y(\beta)}{VH(\beta)}-\frac{\sigma_y(\alpha_0)}{VH(\alpha_0)}}{m_\alpha-1}(i-1)\right]$$

$$i=1\ldots m_\alpha$$

$$\sigma_y(\gamma_{Ii})=VH(\gamma_{Ii})\left[\frac{\sigma_y(\gamma_{II})}{VH(\gamma_{II})}+\frac{\frac{\sigma_y(\beta)}{VH(\beta)}-\frac{\sigma_y(\gamma_{II})}{VH(\gamma_{II})}}{m_{\gamma_I}-1}(i-1)\right]$$

$$i=1\ldots m_{\gamma_I}$$

$$\sigma_y(\gamma_{IIIi})=VH(\gamma_{IIIi})\left[\frac{\sigma_y(\gamma_{II})}{VH(\gamma_{II})}+\frac{\frac{\sigma_y(M)}{VH(M)}-\frac{\sigma_y(\gamma_{II})}{VH(\gamma_{II})}}{m_{\gamma_{III}}-1}(i-1)\right]$$

$$i=1\ldots m_{\gamma_{III}}$$

$$\sigma_y(\gamma_i)=VH(\gamma_i)\left[\frac{\sigma_y(\gamma_0)}{VH(\gamma_0)}+\frac{\frac{\sigma_y(M)}{VH(M)}-\frac{\sigma_y(\gamma_0)}{VH(\gamma_0)}}{m_\gamma-1}(i-1)\right]$$

$$i=1\ldots m_\gamma$$

where $\sigma_{\gamma_{II}}$= yield stress of γ_{II} layer.

Finally, the tensile strength of the $\alpha\beta\gamma M\gamma$ composite is

$$\sigma_{ts}(\alpha\beta\gamma M\gamma)=\sum_{i=1}^{m}VH(\alpha_i)\left[\frac{\sigma_y(\alpha_0)}{VH(\alpha_0)}+\frac{\frac{\sigma_y(\beta)}{VH(\beta)}-\frac{\sigma_y(\alpha_0)}{VH(\alpha_0)}}{m_\alpha-1}(i-1)\right]\left[\frac{\varepsilon'}{\varepsilon(\alpha_i)}\right]^{n(\alpha_i)}V_i+\sigma'(\beta)V(\beta)$$

$$+\sum_{i=1}^{m_{\gamma_I}}VH(\gamma_{Ii})\left[\frac{\sigma_y(\gamma_{II})}{VH(\gamma_{II})}+\frac{\frac{\sigma_y(\beta)}{VH(\beta)}-\frac{\sigma_y(\gamma_{II})}{VH(\gamma_{II})}}{m_{\gamma_I}-1}(i-1)\right]\left[\frac{\varepsilon'\times E}{\varepsilon(\gamma_{Ii})}\right]^{n(\gamma_{I}i)}V_i+\sigma'(\gamma_{II})V(\gamma_{II})$$

$$+\sum_{i=1}^{m_{\gamma_{III}}}VH(\gamma_{IIIi})\left[\frac{\sigma_y(\gamma_{II})}{VH(\gamma_{II})}+\frac{\frac{\sigma_y(M)}{VH(M)}-\frac{\sigma_y(\gamma_{II})}{VH(\gamma_{II})}}{m_{\gamma_{III}}-1}(i-1)\right]\left[\frac{\varepsilon'}{\varepsilon(\gamma_{IIIi})}\right]^{n(\gamma_{III}i)}V_i+\sigma'(M)V(M)$$

$$+\sum_{i=1}^{m_\gamma}VH(\gamma_i)\left[\frac{\sigma_y(\gamma_0)}{VH(\gamma_0)}+\frac{\frac{\sigma_y(M)}{VH(M)}-\frac{\sigma_y(\gamma_0)}{VH(\gamma_0)}}{m_\gamma-1}(i-1)\right]\left[\frac{\varepsilon'}{\varepsilon(\gamma_i)}\right]^{n_{\gamma i}}V_i$$

Table IV. Comparison between Experimental and Calculated Tensile Strength of the Studied Composites

Composite Type	Experimental Results (MPa)	Calculated Results (MPa)
$\alpha\beta\gamma$	596	623
$\gamma M\gamma$	760	773
$\alpha\beta\gamma\beta\alpha$	668	684
$\gamma\beta\alpha\beta\gamma$	681	697
$\alpha\beta\gamma M\gamma$	740	798

If the thickness of each element in regions α, γ_1, γ_{III}, and γ is chosen as 10 μm, considering the number of elements in each region (m_α, $m\gamma_I$, $m\gamma_{III}$, m_γ) and by applying the numerical method, the tensile strength of the $\alpha\beta\gamma M\gamma$ composite is determined and the obtained result is shown in Table IV.

The tensile strength of $\gamma\beta\alpha\beta\gamma$ and $\alpha\beta\gamma\beta\alpha$ composites also has been determined. For the purpose of modeling the $\gamma\beta\alpha\beta\gamma$ composite, a thin ferretic layer is assumed in the middle of the α region. The microhardness of this layer is similar to the alfa steel (α_0); in the previous work,[3] it has been shown that the composition of this layer is similar to the alfa steel. Therefore, the stress-strain behavior of the alfa steel was substituted for that of the assumed α layer in the $\gamma\beta\alpha\beta\gamma$ composite.

Since the minimum microhardness of the γ layer is close to that of the γ_{II} layer in the $\alpha\beta\gamma M\gamma$ composite, given the acceptable similarity between their chemical compositions,[3] the corrected stress-strain curve of the γ_{II} layer was also substituted for the γ layer in the model.

The experimental and calculated tensile strengths for the studied composites are shown in Table IV; despite the assumptions and simplifications considered throughout the process of modeling FGS, there is good agreement between the experimental and calculated results. This could be essentially due to the gradual change of composition in FGSs, leading to the proximity of the mechanical properties of the adjacent elements, since some of the discrepancies observed in modeling certain laminated composites are due to characteristics of the interface or the large difference between the strength or Poisson's ratio of the adjacent elements.

From a design point of view, analogous to some engineering laminated composites,[10] if the uniform distribution of strain in the stressed specimen is essential, the FGS would be fabricated in a symmetrical manner (*e.g.,* $\alpha\beta\gamma\beta\alpha$, $\gamma M\gamma$, and $\gamma\beta\alpha\beta\gamma$).

IV. CONCLUSIONS

1. The tensile strength of FGSs depends on the type and number of layers in the composite.
2. The tensile strengths of FGSs are modeled regarding the tensile properties of the merging bainite and martensite phases in addition to the microhardness profiles of ferritic and austenitic layers based on the rule of mixtures.
3. The obtained results from the proposed model are in good agreement with the experimental results, despite all assumptions and approximations.

ACKNOWLEDGMENTS

The authors express their gratitude to Mr. S. Maysami Azad, Mr. H. Mosaviaghdass, and Miss S. Golbaz for their contribution to this work.

REFERENCES

1. S. Suresh and A. Mortensen: *Int. Mater. Rev.*, 1997, vol. 42, pp. 85-116.
2. J. Askill and D.H. Tolmin: *Phil. Mag.*, 1965, vol. 11, pp. 467-74.
3. J. Aghazadeh Mohandesi and M.H. Shahosseinie: *Metall. Mater. Trans. A*, 2005, vol. 36A, pp. 3471-76.
4. H.E. Pettermann: *Mater. Sci. Eng., A*, 2000, vol. 276, pp. 277-82.
5. A. Berezovski and G.A. Maugin: *Eur. J. Mech., A/Solids*, 2003, vol. 22, pp. 257-65.
6. S. Widjaya and Sujanto: *Thin Solid Films*, 2003, vol. 434, pp. 216-27.
7. Ma and Lin: *Mater. Sci. Forum*, 2003, vols. 423–425, pp. 731-36.
8. A.W. Bowen and P.G. Partridge: *J. Phys.: Appl. Phys.*, 1974, vol. 7, pp. 969-77.
9. D.C. Ludwigson and J.A. Berger: *The Metallurgical Evolution of Stainless Steels*, ASM, Metals Park, OH, 1979, pp. 413-19.
10. B. Ilschner: *J. Mech. Phys. Solids*, 1996, vol. 44, pp. 647-56.